Fuselage Vibration Reduction of Lift-Offset Coaxial Rotor Vehicles with Auxiliary Propulsion via Individual Blade Pitch Control (IBC)

Isabella Mawry, The Pennsylvania State University, State College, PA, USA
Edward Smith, The Pennsylvania State University, State College, PA, USA
Sven Schmitz, The Pennsylvania State University, State College, PA, USA
Jianhua Zhang, The Pennsylvania State University, State College, PA, USA
Jae-Sang Park, Chungnam University, Daejeon, South Korea

Abstract

The present study investigates the fuselage vibration reduction potential for a lift-offset coaxial rotor vehicle with auxiliary propulsion using open-loop individual blade pitch control (IBC) applied to the main rotor. The comprehensive aeroelastic software, Rotorcraft Comprehensive Analysis System (RCAS), was utilized to implement the XH-59A elastic-line fuselage model and create a comprehensive coupled rotor-fuselage model for analysis. An open-loop IBC phase sweep was applied to the main rotor at 200 knots and reduced the 3/rev and 6/rev hub loads and cockpit vibrations. For a 3/rev, $1°$ IBC amplitude at $270°$ phase, the reductions in the 3/rev hub loads for this input were 89% in M_y, 48% in F_z, and 79% in F_x. Additionally, the cockpit vibrations decreased by 81% in the longitudinal direction and 76% in the vertical direction for the 3P/$1°$/$270°$ IBC input. The 6/rev hub loads and cockpit vibrations were also reduced with various open-loop IBC inputs.

1. NOTATION

Symbols

A	IBC pitch amplitude, deg
$F_{x/y/z}$	Rotor hub force, lb
M_x	Rolling moment, lb-ft
M_y	Pitching moment, lb-ft
M_z	Yawing moment, lb-ft
N	IBC harmonic, /rev
N_b	Number of blades per rotor
R	Rotor radius, ft
T	Rotor thrust, lb
V_∞	Flight speed, knots
W	Weight, lb
β_p	Precone angle, deg
ψ	Blade azimuth angle, deg
θ_{IBC}	IBC input angle, deg
φ	IBC phase angle, deg
Ω, Ω_{TR}	Main rotor speed of rotation, rad/s
$()_{3P}$	3/rev harmonic component

Acronyms

IBC	Individual Blade Pitch Control
LO	Lift-offset
RCAS	Rotorcraft Comprehensive Analysis System

2. INTRODUCTION

The development of future vertical lift aircraft pushes the limits of performance and innovation, particularly in achieving high speeds as compared to conventional helicopters. Advanced configurations such as coaxial rotors, tiltrotors, and compound helicopter designs with additional power sources are engineered to attain these high forward flight speeds. However, these high speeds, coupled with the stiff rotor blades, generate significant vibratory loads. In the mid-1970s, Sikorsky Aircraft developed and tested the XH-59A experimental coaxial compound helicopter, which achieved a maximum maneuver envelope of 240 knots with the inclusion of auxiliary propulsion systems (Ref. 11). Notably, it was the first rotary wing aircraft to reach this speed without reliance on an auxiliary wing. Despite its success in reaching these high speeds, the XH-59A demonstrator was ultimately not produced due to excessive vibrations observed during the test program (Ref. 8).

The XH-59A Technology Demonstrator was later succeeded by the X2, which featured advancements in blade construction, propulsion integration, composite material applications, and most importantly for this study, vibration control methods and a fly-by-wire control system (Ref. 8). In early 2010, the X2 reached a top cruise speed of 250 knots, marking a 15% improvement of the record top speed of a conventional helicopter (Ref. 3). The first application of this technology was the S-97 Raider, which was considered for the U.S. Army's Future Attack Reconnaissance Aircraft (FARA) program. The evolution of these designs is shown in Figure 1.

Figure 1. Evolution of Lift-Offset Coaxial Rotor Vehicles with Auxiliary Propulsion. From top to bottom: XH-59A, X2, S-97 (Ref. 11, Ref. 12).

Effective vibration control systems are essential for the safe operation of high-speed vehicles to prevent fatigue to the vehicle structure and its operators. Since the demonstration of the XH-59A, which experienced severe vibrations during test flights, vibration analysis for these aircraft has evolved significantly, leading to the inclusion of active vibration control in the X2 Technology Demonstrator. While the active vibration control system (AVCS) applied to the X2, S-97, and other compound helicopter designs have successfully reduced operational vibrations, these systems are extremely heavy, thus increasing the vehicle's parasitic weight.

Alternative methods of vibration control have been explored to assess the potential of vibration reduction. Individual blade pitch control (IBC) has been investigated for its potential to reduce vibrations while eliminating the need for a heavy system since pitch actuation is already present on the aircraft. The present research focuses on assessing the potential of fuselage vibration reduction through the implementation of IBC on a lift-offset coaxial rotor vehicle using the aeroelastic analysis tool, Rotorcraft Comprehensive Analysis System (RCAS). Previous studies have evaluated the vibratory loads reduction potential of the XH-59A rotor utilizing CAMRAD II aeromechanical software (Ref. 7); this study provided a basis for analytical comparison with the vibratory loads reduction potential of rotor hub loads as predicted by RCAS. The RCAS rotor hub loads and lift-to-drag ratios were successfully validated against the CAMRAD II predictions for baseline studies without the application of vibration control (Ref. 2). Open-loop harmonic IBC actuations were also applied to the main rotor in CAMRAD II and were validated for 2/rev and 3/rev harmonic actuations.

This research aims to investigate the fuselage vibration reduction capabilities of individual blade pitch control (IBC) for lift-offset coaxial rotor vehicles with auxiliary propulsion. Previous studies established the necessary infrastructure for examining IBC on a lift-offset coaxial main rotor. RCAS simulations of the XH-59A rotor with open-loop and closed-loop IBC inputs were analyzed and validated using a prescribed wake aerodynamic model (Ref. 1 and Ref. 2). Additionally, open-loop and closed-loop IBC studies were conducted in RCAS using the Viscous Vortex Particle Method (VVPM) inflow model to improve upon the prediction accuracy at low operating speeds. Using VVPM inflow predicted higher baseline 3/rev and 6/rev hub loads at low and high speeds as compared to the prescribed wake model predictions (Ref. 13).

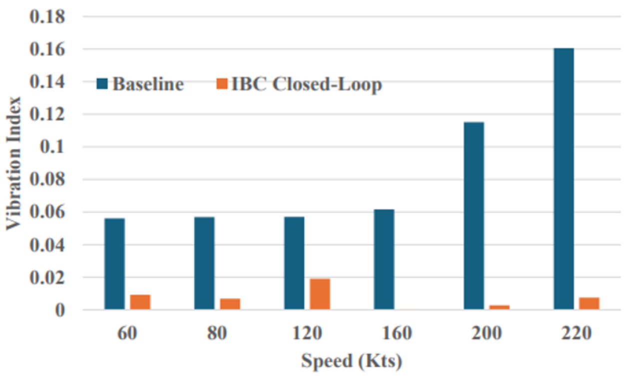

Figure 2. Vibration Index and Percentage Reduction vs. Airspeed [knots] (Ref. 13).

As shown in Figure 2, the vibration index—a non-dimensional value for total rotor hub loads—decreases when closed-loop IBC was applied across airspeeds from 60 to 220 knots (Ref. 13). This illustrated the importance of using VVPM inflow at lower airspeeds for more accurate hub load predictions and defined a 65-95% hub load reduction for various airspeeds through implementing closed-loop IBC. This study also quantified the effects of IBC on vibratory hub loads and the effective lift-to-drag ratio of the coaxial rotor to evaluate the hub loads reduction and performance enhancement potential of this active vibration control technique (Ref. 13).

In the present study, the reduction of hub loads and vibrations at specific fuselage locations will be assessed due to open-loop IBC implementation. The airframe points of interest are shown in Figure 3.

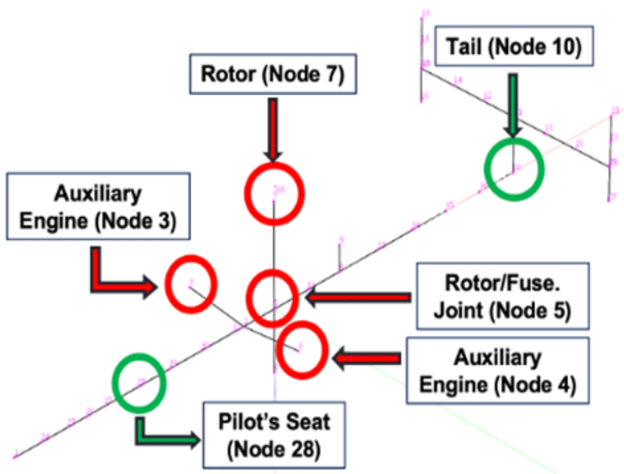

Figure 3. XH-59A Airframe and Analysis Points of Interest.

The baseline vibration predictions and comparisons to the CAMRAD II study will be summarized for an isolated fuselage model in RCAS, and these baseline values will be utilized to evaluate the effectiveness of implementing open-loop IBC on the main rotor for airframe vibration reduction of a coupled rotor-fuselage model. In future work, comparisons of IBC implementation on the main rotor and pusher propeller will be made by assessing the vibration reduction potential. Control authorities and limitation requirements will also be determined in future studies to evaluate the effectiveness of IBC implementation. Furthermore, future research will explore the optimization of active controls and passive fuselage dynamic characteristics. The technical specifications for active propulsor concepts shown in Figure 4, such as stroke and torque requirements, will be assessed.

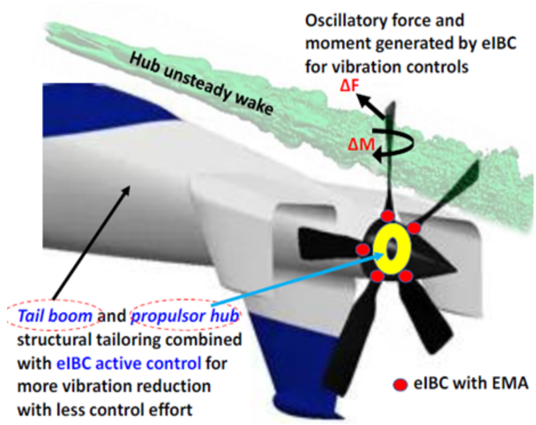

Figure 4. Design space exploration and eIBC active vibration control of the tail boom and propulsor for vibration reduction.

This document summarizes the methodology of the RCAS XH-59A modeling and simulations, current baseline hub loads and vibration results and comparisons, open-loop IBC methodology and results, and future goals.

3. METHODOLOGY

3.1. XH-59A Isolated Fuselage Model

For the analyses, an elastic-line model of the XH-59A airframe was implemented into RCAS, utilizing an existing NASTRAN model developed by Dr. Jae-Sang Park et al. of Chungnam University. The elastic-line model was generated in the NASTRAN finite element software, shown in Figure 5. The goal of utilizing this type of model was to improve computation efficiency while maintaining accuracy as compared to the 3-D XH-59A airframe. The geometric and weight properties of the model were obtained from drawings of the 3-D airframe in the public domain and NDARC calculations, respectively (Ref. 4 and Ref. 7).

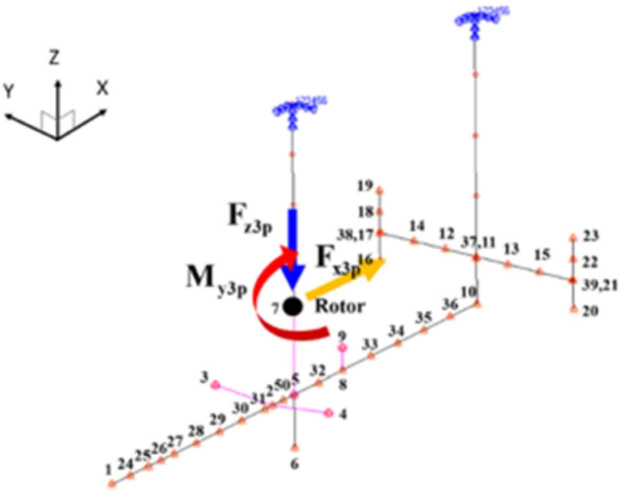

Figure 5. XH-59A Airframe Nodes and Excitations (Ref. 7).

The NASTRAN elastic-line model consisted of 39 finite element nodes. In RCAS, the model finite element coordinates were defined and connected with rigid bars to define the structure. The modal (elastic) structure was superimposed onto the structure by defining the NASTRAN mass and stiffness matrices, and mode shapes of the structure.

To confirm the accuracy of the dynamic properties of the model, the dynamic characteristics were compared to available data of the XH-59A airframe and were deemed similar to proceed with analysis (Ref. 7 and Ref. 10). The dynamic characteristics of the isolated fuselage model are summarized to illustrate the modal contribution of dominant harmonic frequencies. Table 1 shows the model's modes and corresponding natural and excitation frequencies.

Table 1. XH-59A Isolated Fuselage Dynamic Characteristics.

Mode	Natural Frequency [Hz]	Aerodynamic Excitation Frequency
1	3.65	--
2	5.29	--
3	**5.46**	**1/rev**
…	…	--
9	**16.71**	**3/rev**
10	**16.71**	**3/rev**
…	…	--
14	**34.67**	**6/rev**
…	…	--

The natural frequencies closest to the dominant hub loads, 3/rev and 6/rev, are noted as they indicate possible excitation of the fuselage modes when the fuselage is coupled with a rotor system and excited by aerodynamic loading.

3.2. XH-59A Coupled Rotor-Fuselage Model

The isolated fuselage model was coupled with a previously modeled XH-59A rotor system within RCAS (Ref. 1). The rotor system consists of two counter-rotating stiff in-plane hingeless rotors, with each rotor having three blades, $N_b = 3$. Each blade is rigidly attached to the hub and has a pitch bearing for collective, cyclic, and IBC inputs. The structural model of the blades consists of 10 equal-length nonlinear elastic beam elements with flap, lag, and torsional motion. The simulation parameters and rotor and fuselage systems are defined in Table 2.

Table 2. XH-59A Helicopter Parameters.

Characteristic	English	Metric
Fuselage Length	40 ft. 10 in.	12.45 m.
Rotor Radius	18 ft.	5.49 m.
Rotor Separation	30 in.	0.76 m.
# of Rotors	2	--
Blades per Rotor	3	--
Blade Pre-cone	3 deg.	--
Rotor Engines	2 x P&W PT6-3 turboshaft	
Auxiliary Propulsion	2 x P&W J-60-P3A turbojet	
Gross Weight	13,000 lb.	5,897 kg.
Lift-offset	0.25	
Rotor Rotation Rate	345 RPM at 100% RPM	
Rotor Tip Speed	650 ft/s	198.1 m/s

The model was coupled sequentially by adding one rotor to the rotor finite element node (Node 7) in the isolated fuselage model. A massless, rigid bar was defined to connect the second rotor to the first rotor, shown in Figure 6.

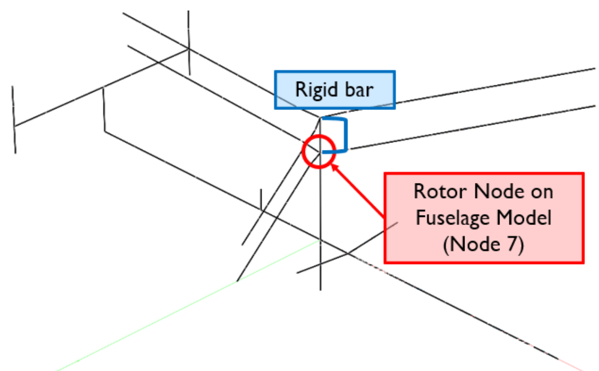

Figure 6. XH-59A Coupled Rotor-Fuselage Structural Model.

An eigenanalysis was performed on both the single-rotor and coaxial rotor coupled models to confirm the proper implementation of the rotor system on the fuselage. The model was then excited with hub loads in the coupled rotor-fuselage configuration. This allows for the translation of the elastic behaviors between the rotor and fuselage subsystems, which is expected to change the responses of the system.

3.3. Aerodynamics

Following the structural coupling of the rotor and fuselage systems, aerodynamic modeling was superimposed on the system. The aerodynamic modeling utilized for these studies is a dual-peaked prescribed vortex wake inflow model. The aerodynamic modeling of the blade included 24 aerodynamic segments. The interference modeling between the rotors was simulated, but it is noted that previous studies using VVPM improved results for simulating complex interactional aerodynamics. The aerodynamic model superimposed on the structural coupled rotor-fuselage model in RCAS is shown in Figure 7.

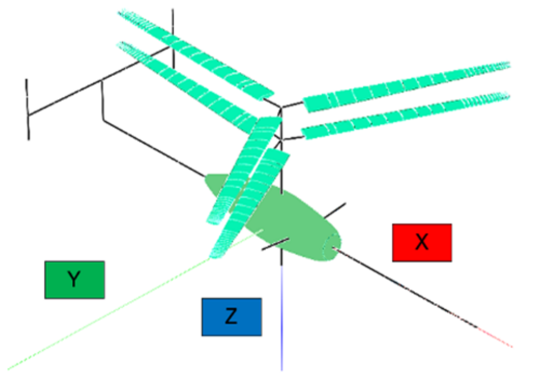

Figure 7. XH-59A Coupled Rotor-Fuselage Model with Aerodynamic Modeling.

The coaxial rotor was trimmed to the weight of the vehicle with the vertical force, F_z, using the upper and lower rotor collective pitch. The rotor was also trimmed to a zero total rotor torque, with the yaw moment, M_z, trimmed to zero using the differential collective. The longitudinal cyclic inputs were utilized to trim the rotor to zero pitching moment, M_y. Lastly, the lateral cyclic inputs were used to trim the roll moment, M_x, to a target value, which was dependent upon a specified lift-offset (LO) value, thrust (T), and rotor radius (R), as described in Eq. 1.

(1) $$M_x = LO \cdot T \cdot R$$

The resulting six trim controls used for this set-up are represented in Figure 8 for a range of airspeeds [knots]: mean and differential collectives and longitudinal and lateral cyclics for the upper and lower rotors. The trim controls for the coupled rotor-fuselage model were comparable to the resulting controls from the isolated coaxial rotor studies, as expected (Ref. 1).

The resulting magnitudes of the vibratory hub forces

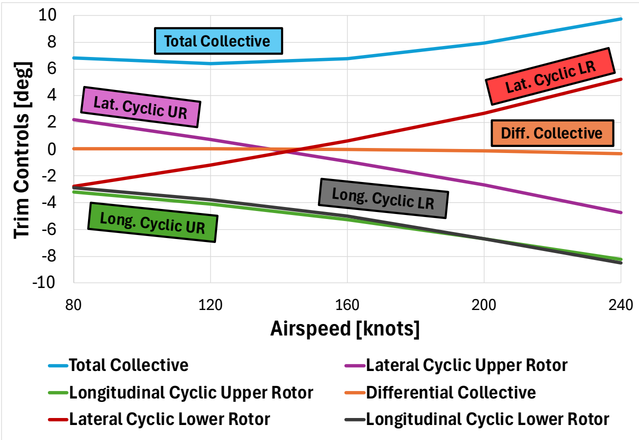

Figure 8. XH-59A Coupled Rotor-Fuselage Trim Controls.

and moments of the coaxial main rotor from the coupled rotor-fuselage simulations are defined by the calculations in Eq. 2 and Eq. 3.

(2) $$F_{3P} = \sqrt{(F^{upper}_{3P,cos} + F^{lower}_{3P,cos})^2 + (F^{upper}_{3P,sin} + F^{lower}_{3P,sin})^2}$$

(3) $$M_{3P} = \sqrt{(M^{upper}_{3P,cos} + M^{lower}_{3P,cos})^2 + (M^{upper}_{3P,sin} + M^{lower}_{3P,sin})^2}$$

Each rotor system has three blades; therefore, the dominant hub loads are 3/rev and 6/rev harmonics for the coaxial rotor configuration. In Eq. 2 & Eq. 3, the 3/rev harmonic hub load components are indicated by F_{3P} and M_{3P}. The cosine and sine components are each summed for the upper and lower rotors. The magnitude of the resulting coaxial hub load is calculated by summing the squares of the cosine and sine components. This process can be repeated for each axis direction, (x, y, z), and other harmonics.

3.4. Open-Loop IBC Implementation

Individual blade pitch control (IBC) is applied to the coaxial rotor system for the coupled rotor-fuselage system as a periodic pitch input on the pitch bearing of each rotor blade. The periodic IBC pitch input, θ_{IBC}, is defined in Eq. 4 with inputs defined as follows: IBC pitch amplitude (A), IBC harmonic (N), blade azimuth (ψ), and IBC phase (φ).

(4) $$\theta_{IBC} = A \cdot \cos(N\psi - \varphi)$$

An example of defined IBC inputs is as follows: 4P/1°/0°, which means that there is a 4/rev IBC harmonic, 1° pitch amplitude, and 0° phase angle. The baseline studies used as a comparison for the IBC studies utilized the coupled rotor-fuselage model responses to the same aerodynamic excitations with no control inputs.

A reference system within RCAS was defined for the periodic input, with the upper rotor rotational rate defined as the reference. The upper rotor rotates counterclockwise, a positive rotational rate in RCAS, shown in Figure 9. Both rotors define a zero azimuth, $\psi = 0$, as pointing towards the tail. The rotor rotational directions are also shown in Figure 9 for the upper rotor, Ω_U, and lower rotor, Ω_L.

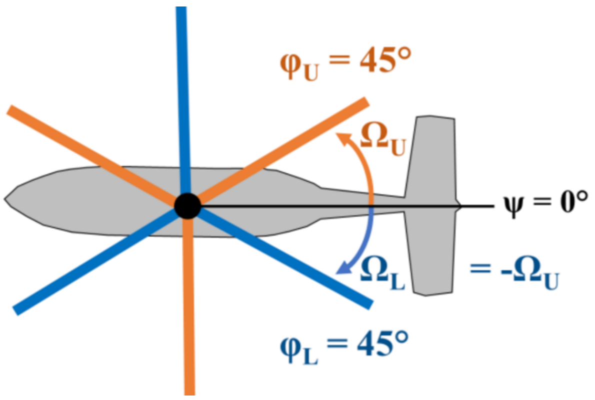

Figure 9. XH-59A Upper and Lower Rotors Rotational Directions.

4. RESULTS AND DISCUSSION

4.1. Baseline Hub Loads and Vibrations

The baseline hub loads of the coupled rotor-fuselage model were defined to compare to previous studies with the isolated coaxial rotor, as well as provide baseline hub load values as a comparison to the resulting loads when IBC is implemented on the rotor.

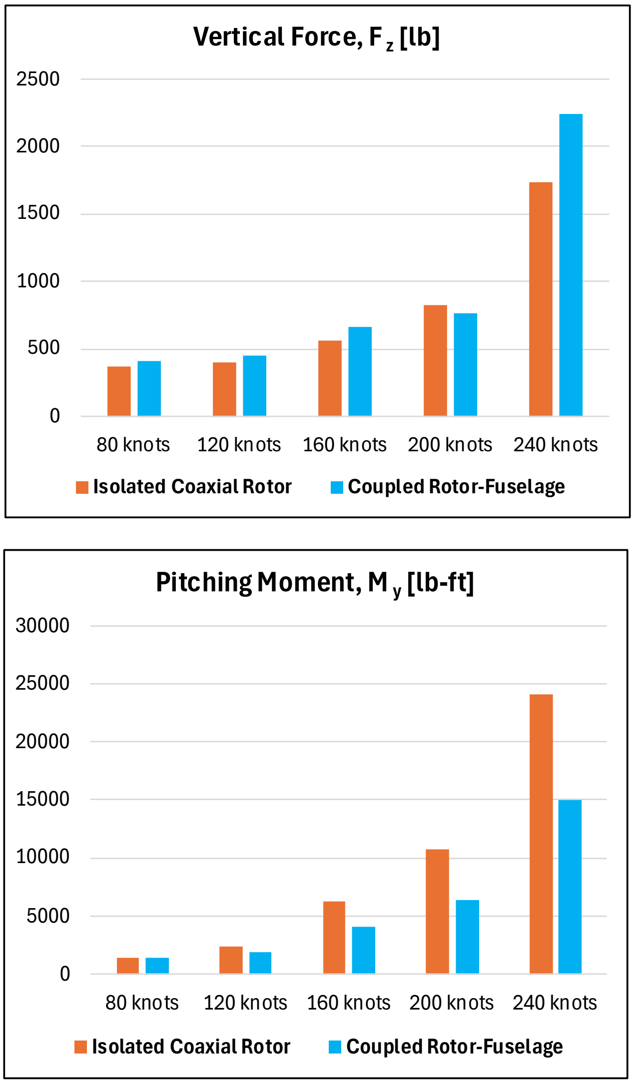

Figure 10. 3/rev Vertical Force [lb] and Pitching Moment [lb-ft] for Isolated Coaxial Rotor (Ref. 1) and Coupled Rotor-Fuselage Models for a range of Airspeeds [knots].

The resulting hub loads as compared to the isolated rotor hub loads from previous studies are shown in Figure 10. The vertical force and pitching moment are the most significant hub loads for this configuration.

The trimmed hub loads for the coupled rotor-fuselage configuration are sensitive to speed changes, where the hub loads increase with speed, as expected. Figure 10 also shows the sensitivity of the hub loads to the model configuration, which illustrates the importance of utilizing a coupled rotor-fuselage model for defining the resulting hub loads of a complete helicopter system. Additionally, for high speeds greater than 160 knots, there are more significant differences in the resulting hub load magnitudes.

The 6/rev hub loads for the coupled rotor-fuselage configuration were also recorded to illustrate the importance of incorporating these excitations in the studies. Figure 11 shows the resulting 6/rev hub loads for the isolated rotor (Ref. 1) and the coupled rotor-fuselage configuration for a range of airspeeds.

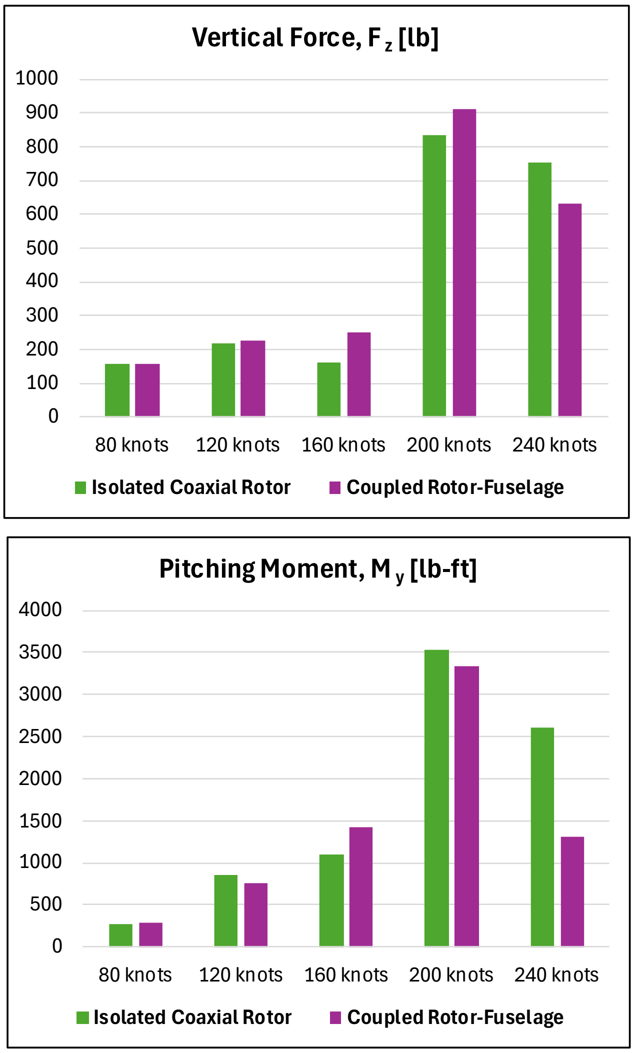

Figure 11. 6/rev Vertical Force [lb] and Pitching Moment [lb-ft] for Isolated Coaxial Rotor (Ref. 1) and Coupled Rotor-Fuselage Models for a range of Airspeeds [knots].

As shown in Figure 11, the resulting 6/rev hub loads for both the isolated coaxial rotor and coupled rotor-fuselage configurations are significant in magnitude and should also be considered for the reduction in hub loads utilizing IBC inputs.

Following the quantification of the dominant hub loads for the coupled rotor-fuselage configuration, the baseline airframe vibrations were defined for the system. The cockpit location on the airframe is utilized as the main point of interest for the vibration studies, as there is analytical and flight test data for comparison of results.

The isolated fuselage model was excited using the trimmed hub loads of the isolated rotor model from previous studies (Ref. 1). The coupled rotor-fuselage vibrations were compared to the isolated fuselage model vibrations to assess the importance of using a coupled model for defining responses. Figure 12 shows the comparison of vibrations for both configurations for a range of airspeeds.

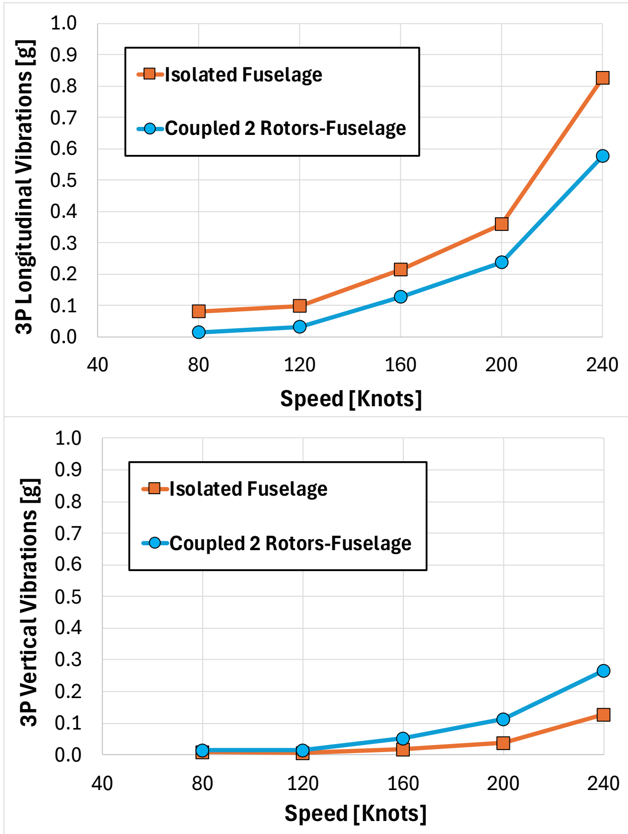

Figure 12. 3/rev Cockpit Long. and Vertical Vibrations [g] for Isolated Fuselage and Coupled Rotor-Fuselage Models vs. Airspeeds [knots].

The comparison of the longitudinal and vertical vibrations for both model configurations also illustrated the importance of using a coupled model for analysis. The resulting vibrations in the longitudinal and vertical directions were also compared to existing analytical studies and flight test data.

Figure 13 shows the current comparison of the isolated fuselage vibration responses to the isolated rotor hub load excitations, the coupled rotor-fuselage responses to aerodynamic excitations, the CAMRAD II study (Ref. 7), and flight test data points (Ref. 6 and Ref. 10).

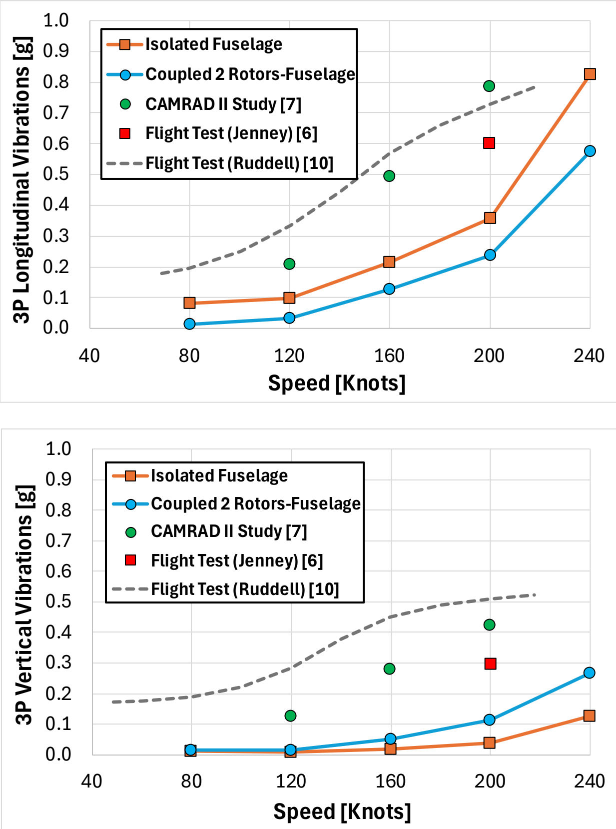

Figure 13. 3/rev Cockpit Longitudinal and Vertical Vibrations [g] versus Airspeed [knots] for the isolated fuselage, the coupled rotor-fuselage responses to aerodynamic excitations, the CAMRAD II study (Ref. 7), and flight test data points (Ref. 6 and Ref. 10).

As shown in Figure 13, the longitudinal and vertical vibrations of the vehicle's cockpit are significant in magnitude. This reaffirms the need for a control system to minimize vibrations of the vehicle for safe operation. The resulting vibrations of the current study, for the isolated fuselage model and coupled rotor-fuselage model, slightly underpredict the vibrations compared to the flight test data and analytical data. Open-loop IBC inputs will be applied to the main rotor to assess the effect of reducing these vibrations at the cockpit to aid in the vehicle's safe operation.

4.2. Open-Loop IBC

Open-loop IBC inputs were first applied to assess the effect on the hub loads and vibrations as compared to the baseline results. A range of open-loop IBC inputs were defined for the current studies. $(N-1)/rev$, N/rev, and $(N+1)/rev$ harmonics for $N=3$ and $N=6$ were utilized in these studies to assess the change in the 3/rev and 6/rev vibratory hub loads, respectively, and fuselage vibrations for various harmonics. Additionally, the harmonic phase was changed for a range of $\varphi = 0° - 315°$. The pitch amplitude was also changed for these studies. With the variation of these IBC parameters, the effectiveness in reducing the hub loads and fuselage vibrations was assessed at 200 knots.

Figure 14 shows the resulting 3/rev hub load magnitudes for $1°$ and $0.5°$ pitch amplitudes. The 3/rev pitching moment, M_y, vertical force, F_z, and longitudinal force, F_x hub loads were presented as they are the main loads acting on the system due to the defined $\psi = 0$ cross-over angle of the rotors. According to Figure 14, 3P/$1°/270°$ for $1°$ pitch amplitudes and 3P/$0.5°/270°$ for $0.5°$ pitch amplitudes are the most effective in reducing the respective hub loads. The $1°$ pitch amplitude results are the most significant decrease in the longitudinal force and pitching moment responses. Applying a 3P/$1°/270°$ IBC input resulted in an 89% decrease in the pitching moment, a 48% decrease in the vertical force, and a 79% decrease in the longitudinal force. This illustrates that implementing open-loop IBC inputs on the main rotor system can reduce the resulting 3/rev hub loads.

The 6/rev hub loads were deemed significant in magnitude for both the isolated rotor and coupled rotor-fuselage configurations. Open-loop IBC was also applied to target minimizing the 6/rev hub loads of the coupled rotor-fuselage model with 5/rev, 6/rev, and 7/rev IBC harmonic frequencies for $1°$ and $0.5°$ pitch amplitudes. Figure 15 shows the resulting 6/rev hub loads with the applied open-loop IBC inputs. For a $1°$ pitch amplitude, the resulting pitching moment had the largest decrease in magnitude for a 7P/$1°/225°$ IBC input, with a 73% decrease in magnitude. The vertical force had a maximum decrease of 89% for an input of 5P/$1°/270°$. For a $0.5°$ pitch amplitude, the resulting pitching moment had the largest decrease in magnitude for a 5P/$0.5°/270°$ IBC input, with a 93% decrease in magnitude. The vertical force had a maximum decrease of 89% for an input of 6P/$0.5°/315°$. The largest 6/rev hub loads, the pitching moment, M_y, and vertical force, F_z, can be reduced by implementing open-loop IBC inputs on the main rotor system.

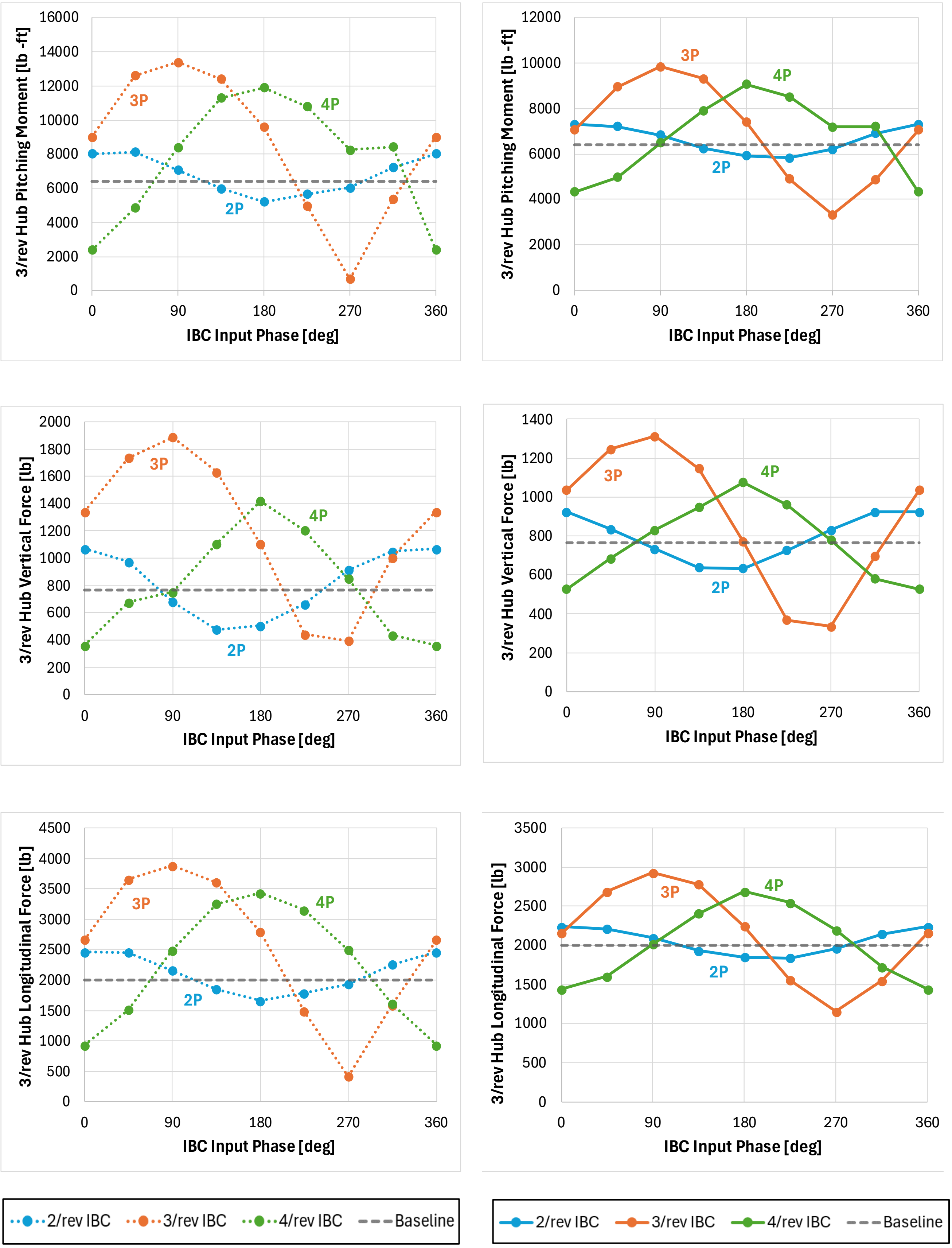

Figure 14. 3/rev Coupled Rotor-Fuselage Hub Loads Responses to Open-loop IBC Inputs at 200 Knots.
Left: 1° IBC Pitch Amplitude, **Right:** 0.5° IBC Pitch Amplitude

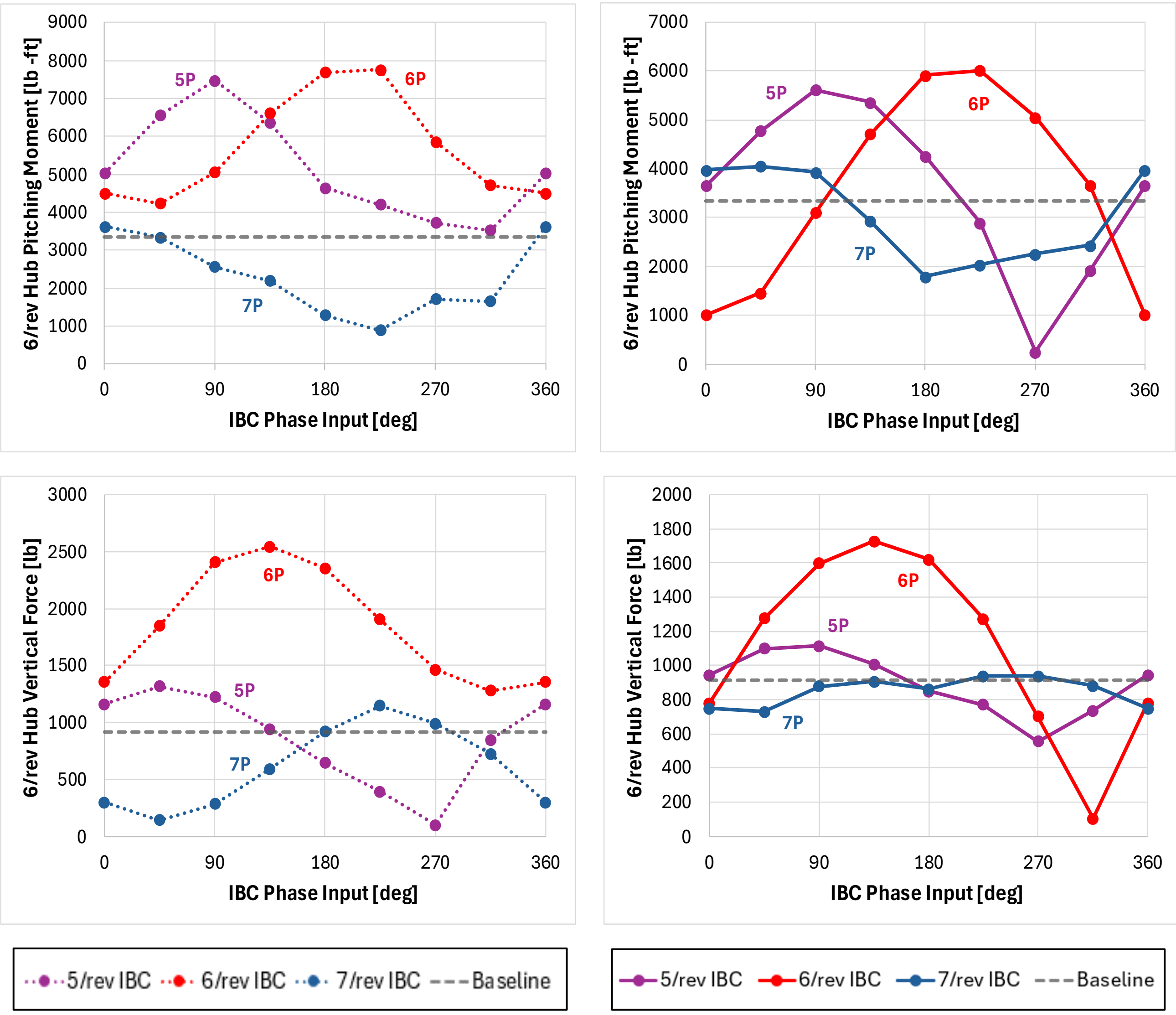

Figure 15. 6/rev Coupled Rotor-Fuselage Hub Loads Responses to Open-loop IBC Inputs at 200 Knots.
Left: 1° IBC Pitch Amplitude, **Right:** 0.5° IBC Pitch Amplitude

The open-loop IBC input for the coupled rotor-fuselage model that resulted in the maximum reduction in the hub loads differed from previous studies using the isolated rotor model (Ref. 2). For the coupled rotor-fuselage model, the IBC inputs that resulted in the maximum reduction of the 3/rev hub loads were 3/rev harmonic inputs with a 270° phase input for each pitch amplitude; the best-case IBC inputs from previous studies for the isolated rotor were 4/rev harmonic inputs with a 0° phase input. A summary of the best-case open-loop IBC inputs for minimizing the 3/rev hub loads of the coupled rotor-fuselage model are shown in Figure 16, where there is a comparison of the effect of applying the best-case inputs from the previous studies to the coupled rotor-fuselage model versus the best-case inputs for the current model.

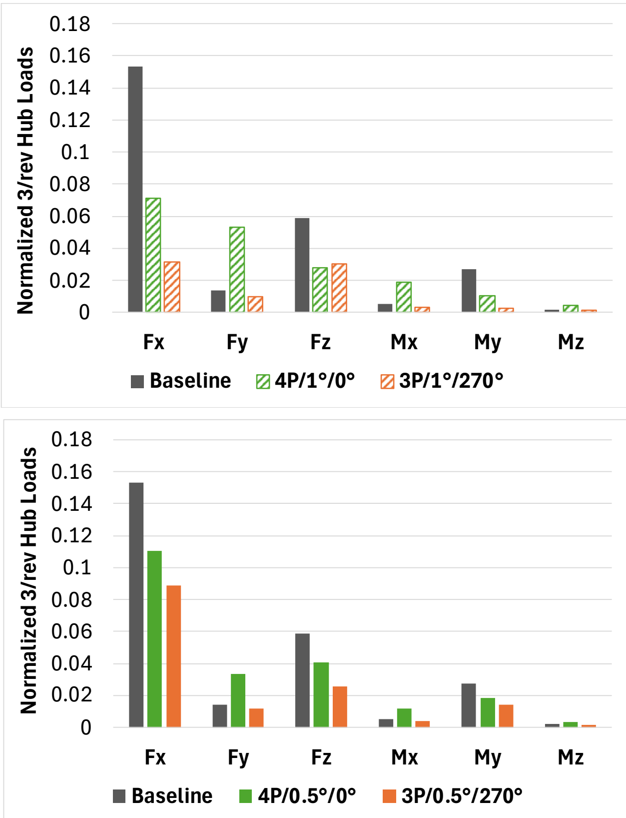

Figure 16. Normalized 3/rev Hub Loads for Open-Loop IBC Inputs Applied to Main Rotor on Coupled Rotor-Fuselage Model at 200 Knots (Forces divided by Vehicle Weight, Moments divided by Weight and Rotor Radius).

The open-loop IBC inputs for minimizing the 6/rev hub loads varied between the individual loads. For example, Figure 17 shows the normalized 6/rev hub loads for various open-loop IBC inputs.

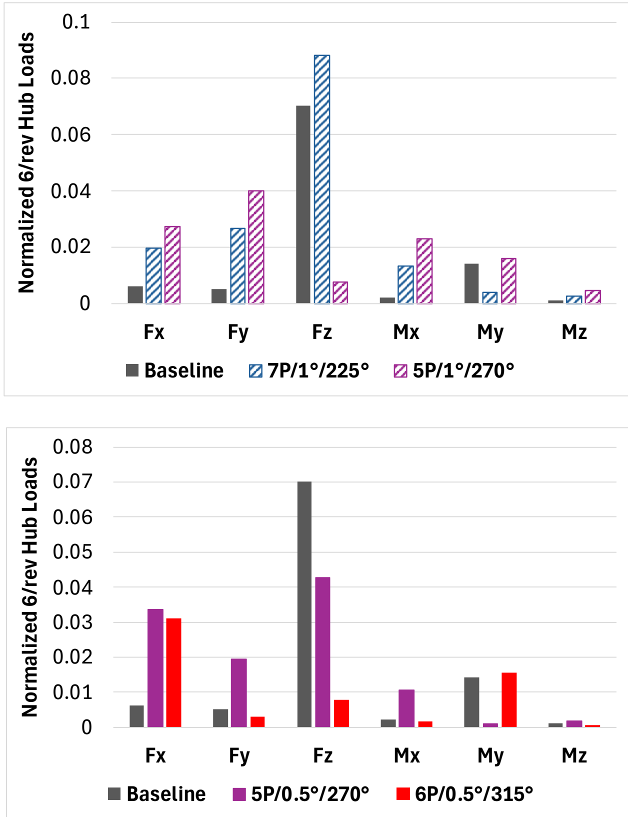

Figure 17. Normalized 6/rev Hub Loads for Open-Loop IBC Inputs Applied to Main Rotor on Coupled Rotor-Fuselage Model at 200 Knots (Forces divided by Vehicle Weight, Moments divided by Weight and Rotor Radius).

The 7P/1°/225° IBC input significantly reduced the pitching moment magnitude but increased the vertical force magnitude in comparison to the baseline value. Additionally, the 5P/1°/270° IBC input significantly reduced the vertical force but increased the pitching moment in comparison to the baseline value.

The 0.5° pitch amplitude IBC inputs also resulted in variations of effectiveness depending upon the hub load investigated, mirroring the difference in the 1° pitch amplitude results. The 6P/0.5°/315° IBC input increased the pitching moment magnitude, while the 5P/0.5°/270° input decreased the pitching moment magnitude. The IBC inputs to reduce the magnitudes of the 6/rev hub loads vary for which load is targeted for minimization. Smaller pitch amplitudes may be necessary to reduce all 6/rev hub loads for a single IBC input. Closed-loop IBC algorithms are needed to target minimizing all hub loads for a particular IBC input and will be utilized in future work.

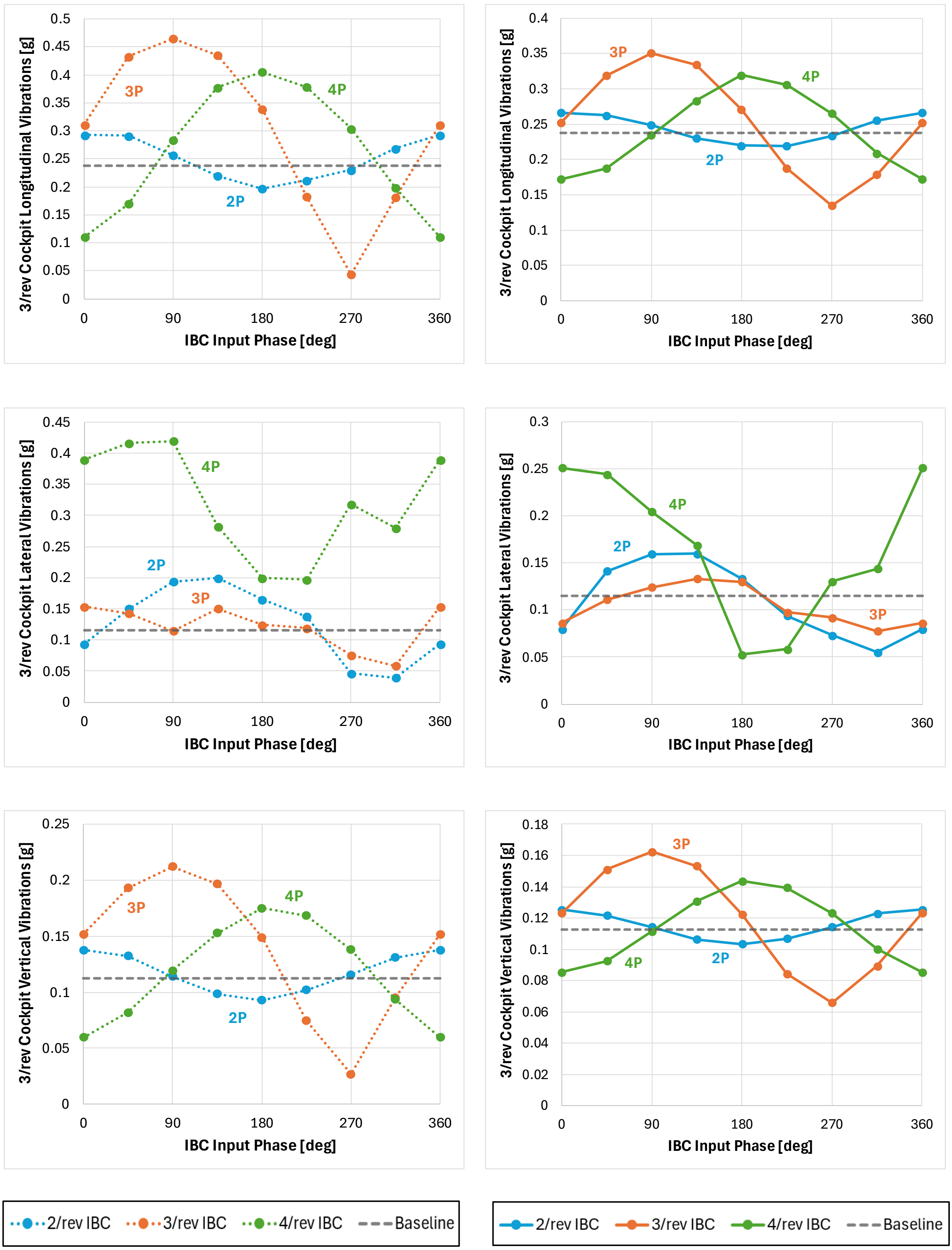

Figure 18. 3/rev Coupled Rotor-Fuselage Cockpit Vibration Responses to Open-loop IBC Inputs at 200 Knots.
Left: 1° IBC Pitch Amplitude, **Right:** 0.5° IBC Pitch Amplitude

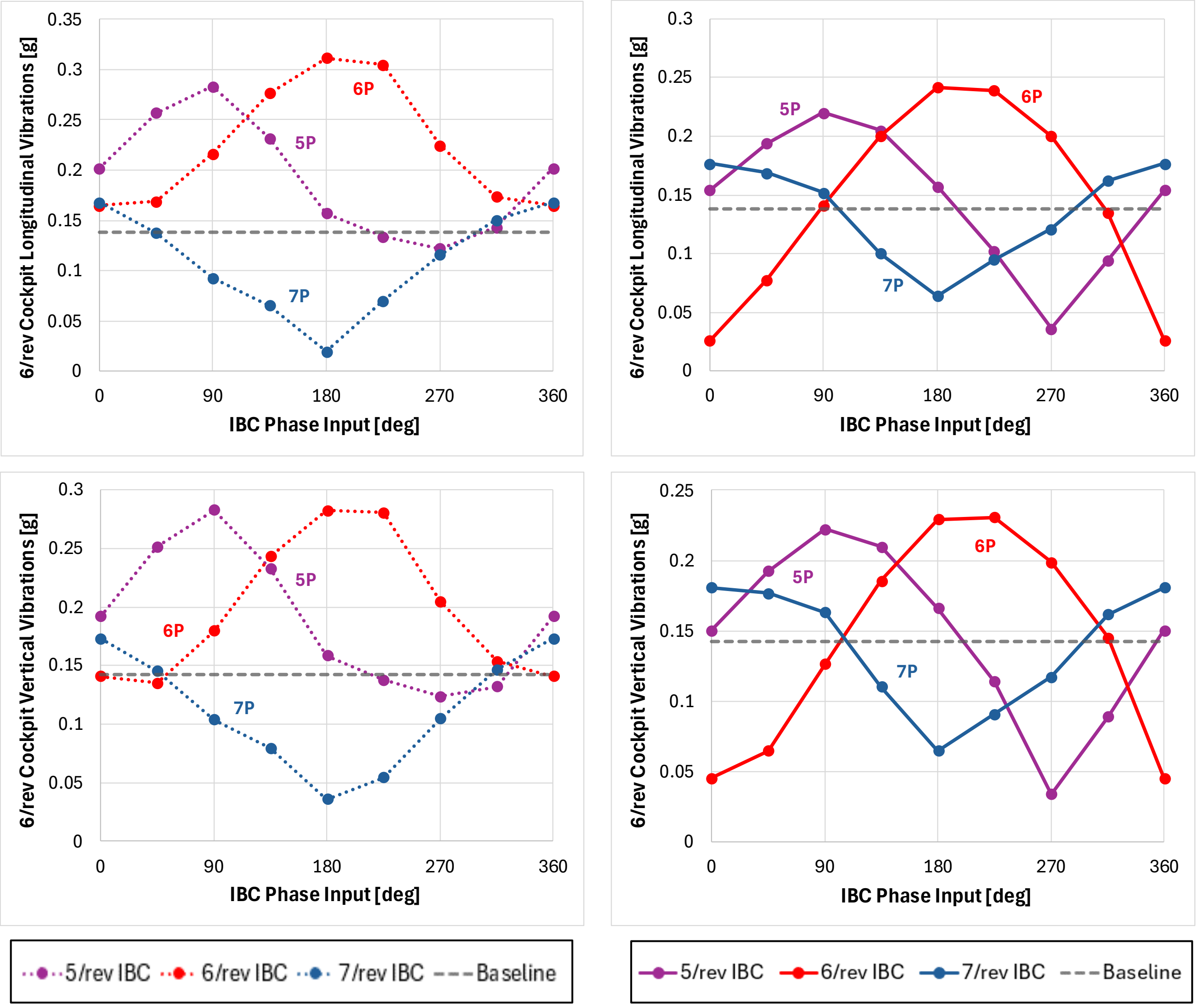

Figure 19. 6/rev Coupled Rotor-Fuselage Cockpit Vibration Responses to Open-loop IBC Inputs at 200 Knots. **Left:** $1°$ IBC Pitch Amplitude, **Right:** $0.5°$ IBC Pitch Amplitude

In addition to investigating the effect of IBC inputs on the 3/rev and 6/rev hub loads, the 3/rev and 6/rev cockpit vibrations were also assessed when open-loop IBC inputs were applied to the main rotor of the coupled rotor-fuselage model in RCAS. Figure 18 shows the 3/rev longitudinal, lateral, and vertical vibrations [g] at the cockpit for an IBC phase sweep [deg] for $1°$ and $0.5°$ pitch amplitudes. The 3P/$1°/270°$ for $1°$ pitch amplitudes and 3P/$0.5°/270°$ for $0.5°$ pitch amplitudes are the most effective in reducing the cockpit's longitudinal and vertical vibration responses. The $1°$ pitch amplitude results in the most significant decrease in the longitudinal and vertical vibration responses. Applying a 3P/$1°/270°$ IBC input resulted in an 81% decrease in the longitudinal vibrations and a 76% decrease in the vertical vibrations at the cockpit.

For the 6/rev cockpit vibrations of the coupled rotor-fuselage model, implementing open-loop IBC inputs on the main rotor reduced the longitudinal and vertical vibrations. Figure 19 shows the effect of $1°$ and $0.5°$ pitch amplitudes for a range of phase and harmonic inputs. The longitudinal vibrations were reduced by 86% and the vertical vibrations were reduced by 75% for an open-loop IBC input of 7P/$1°/180°$. A $0.5°$ pitch amplitude with 6/rev harmonic frequency and $0°$ phase resulted in an 81% reduction in the longitudinal vibrations at the cockpit. A 76% reduction in the vertical vibrations at the cockpit was at a maximum for the 5P/$0.5°/270°$ IBC inputs on the main rotor. This illustrates that implementing IBC inputs on the main rotor system can reduce the resulting 3/rev and 6/rev vibrations significantly and aid in the safe operation of the vehicle.

For the coupled rotor-fuselage model, the vibrations at the cockpit for the longitudinal and vertical directions were large in magnitude. IBC inputs need to be evaluated to minimize these vibrations for the safe operation of lift-offset coaxial rotor vehicles with auxiliary propulsion systems. The open-loop IBC inputs that minimize the cockpit vibrations were investigated for 3/rev and 6/rev harmonics.

The IBC input that resulted in the maximum reduction of the 3/rev cockpit vibrations in the longitudinal, lateral, and vertical directions were 3/rev harmonic inputs with a $270°$ phase input for each pitch amplitude. A summary of the best-case IBC inputs and their effect on the 3/rev cockpit vibrations is shown in Figure 20.

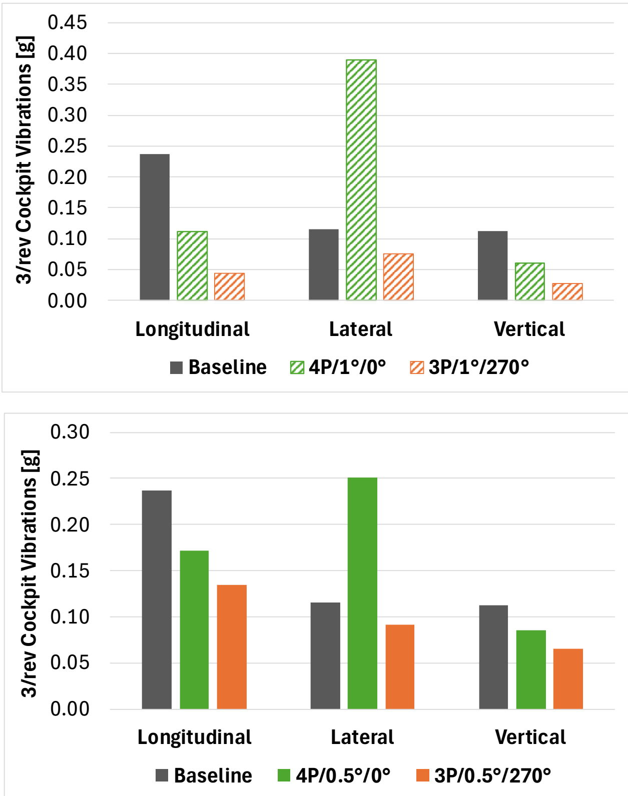

Figure 20. 3/rev Cockpit Vibrations for Open-Loop IBC Inputs Applied to Main Rotor on Coupled Rotor-Fuselage Model at 200 knots.

For the 4/rev harmonic inputs with a $0°$ phase input, the lateral vibrations increase significantly. These inputs were the most successful in reducing the 3/rev hub loads for the isolated rotor model, but once the model was coupled with the elastic fuselage, it became less effective in reducing the 3/rev hub loads and increased the vibrations at the cockpit in the lateral direction.

A summary of the best-case open-loop IBC inputs for minimizing the 6/rev cockpit vibrations of the coupled rotor-fuselage model are shown in Figure 21.

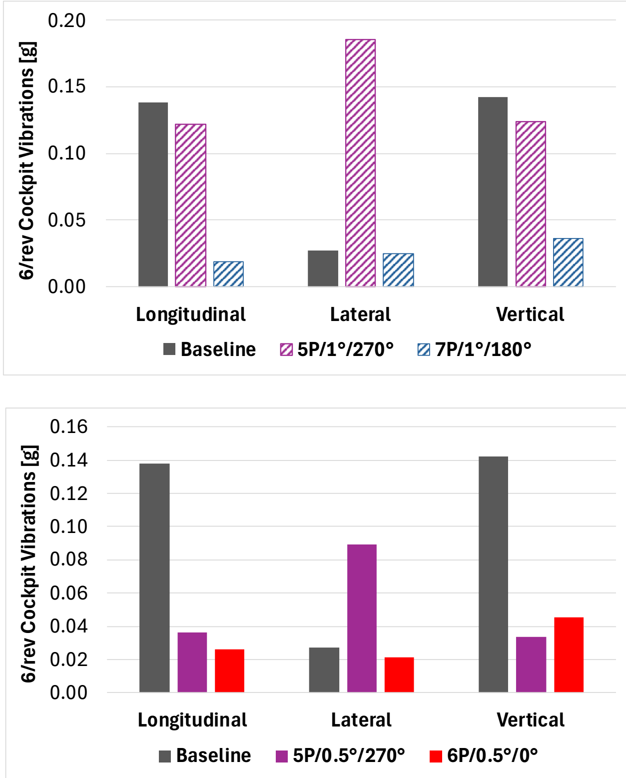

Figure 21. 6/rev Cockpit Vibrations for Open-Loop IBC Inputs Applied to Main Rotor on Coupled Rotor-Fuselage Model at 200 Knots.

The best-case open-loop IBC input for minimizing the 6/rev cockpit vibrations for a $1°$ pitch amplitude was a 7/rev harmonic with a $180°$ phase angle. This input was successful in reducing the cockpit vibrations in all directions of motion. For the 5/rev harmonic with a $270°$ phase angle IBC input, the reduction in the longitudinal and vertical direction is less significant in reference to the baseline values, and there is an increase in the lateral vibrations.

For the $0.5°$ pitch amplitude, 5/rev harmonic with a $270°$ phase angle IBC input, the reduction in the longitudinal and vertical direction is more significant in reference to the baseline values, but there is still an increase in the lateral vibrations. The 6P/0.5°/0° input was successful in reducing the cockpit vibrations in all directions of motion. For the cockpit vibrations, and vibrations at other fuselage locations, a closed-loop control algorithm would also be optimal to maximize the reduction in the vibrations for all directions.

5. CONCLUSIONS

As innovative high-speed, compound helicopters continue development, the high vibratory loading on the vehicles need to be reduced for safe operation. Existing control methods, such as Active Vibration control Systems (ACVS) contribute to the parasitic weight of the vehicle. The proposed control method, Individual Blade Pitch Control (IBC), utilizes existing pitch link actuation to target airframe vibrations.

In the current study, an XH-59A elastic-line fuselage was implemented into the comprehensive aeroelastic software, Rotorcraft Comprehensive Analysis System (RCAS) for vibration analysis. The infrastructure within RCAS was then expanded to couple the XH-59A isolated rotor with the fuselage model. The resulting 3/rev and 6/rev hub loads of the coupled model were defined and compared to the isolated rotor model hub loads using the same aerodynamic inflow model. It was found that the hub loads are sensitive to model configuration, with and without a fuselage model. The 6/rev hub loads were significant in magnitude. Additionally, the 3/rev vibrations of the coupled rotor-fuselage model at the cockpit were defined and compared to existing analytical and flight test data. The 3/rev vibrations of the current study are also sensitive to model configuration.

Open-loop IBC inputs were applied to the main rotor of the coupled rotor-fuselage model to assess the potential decrease in 3/rev and 6/rev hub loads and cockpit vibrations. The resulting 3/rev hub loads and cockpit vibrations saw the most significant decrease in magnitude for the 3P/$1°$/$270°$ IBC input, with an 89% decrease in the pitching moment, a 79% decrease in the longitudinal force, an 81% decrease in the longitudinal vibrations at the cockpit, and a 76% decrease in the vertical vibrations at the cockpit. For the 6/rev hub loads, the optimal IBC inputs varied depending upon the reduction in particular hub loads and did not reduce all hub loads simultaneously.

The resulting reductions in the hub loads and cockpit vibrations almost all depend upon different open-loop IBC inputs, meaning that some inputs may only be effective in reducing particular loads or vibrations in specific directions. With many variations in the most effective open-loop inputs for reducing the hub loads and vibrations at the cockpit, a closed-loop control method is necessary to converge upon the IBC inputs that have a maximum reduction of the hub loads in all directions. Following the convergence of the optimal IBC inputs for maximum hub load reduction, a closed-loop control algorithm must be utilized to converge upon the inputs that will be most effective in reducing the vibrations at various fuselage locations, as the optimal inputs for reducing the hub loads may not be the same as for the reduction of the vibrations in all directions at various fuselage locations.

The application of IBC on the main rotor may not be the most effective and feasible method for maximum reduction of the loading and vibrations on the vehicle. The innovative designs with auxiliary propulsion systems present another location for control applications that may be easier to execute. A comparison of applying IBC with open-loop and closed-loop methods to the pusher propeller versus application on the main rotor system will be made in future studies to quantify technical specifications necessary for the proper actuation of the individual blade pitch control inputs.

Author contact:

Isabella Mawry: irm5116@psu.edu

Edward Smith: ecs5@psu.edu

Sven Schmitz: sus52@psu.edu

Jianhua Zhang: jxz19@psu.edu

Jae-Sang Park: aerotorcraft@gmail.com

6. ACKNOWLEDGMENTS

The authors thank Dr. Louis Centolanza, Dr. Hyeonsoo Yeo, and Dr. Mark Fulton from the U.S. Army Combat Capabilities Development Command, as well as the members of the VLRCOE review team including Mr. William A. Welsh from Sikorsky Aircraft, A Lockheed Martin Company. The authors also would like to thank Hossein and Syna Saberi and Matt Hasbun at Advanced Rotorcraft Technology, Inc. for their guidance with RCAS.

This research is funded by the Government under Cooperative Agreement No. W911W6-21-2-0002. The U.S. Government is authorized to reproduce and distribute reprints for Government purposes notwithstanding any copyright notation thereon. The views and conclusions contained in this document are those of the authors and should not be interpreted as representing the official policies or position, either expressed or implied, of the U.S. Army Combat Capabilities Development Command (DEVCOM), Aviation & Missile Center (AvMC), or the U.S. Government.

7. REFERENCES

1. Beyer, J. “Individual Blade Pitch Control (IBC) for Vibration Reduction of Lift-Offset Coaxial Rotor Vehicles with Auxiliary Propulsion.” *Pennsylvania State University*, 2023.

2. Beyer, J., Smith, E., Schmitz, S., Zhang, J. “Individual Blade Pitch Control (IBC) for Vibration Reduction of Lift-Offset Coaxial Rotor Vehicles with Auxiliary Propulsion.” VFS 79th Annual Forum, West Palm Beach, FL, May 16-18, 2023. Vertical Flight Society, 2023.

3. Connor, R. “Sikorsky X2 Helicopter Reaching New Speeds.” National Air and Space Museum, 2016. https://airandspace.si.edu/stories/editorial/sikorsky-x2-helicopter.

4. Go, J.I., Park, J.S., Choi, J.S. “Validation on conceptual design and performance analyses for compound rotorcrafts considering lift-offset.” Int. J. Aeronaut. Space Sci., 2017.

5. Jacobellis, G. “Improvement of High-Speed Coaxial Rotor Performance Using Redundant Controls and Camber Morphing.” Rensselaer Polytechnic Institute, December 2018.

6. Jenney, D.S. “ABC Aircraft Development Status.” European Rotorcraft and Powered Lift Aircraft Forum, 1980.x

7. Lee, Y., Kim, D., Park, J., Hong, S., “Vibration Reduction Simulations of a Lift-offset Compound Helicopter Using Two Active Control Techniques.” Elsevier Aerospace Science and Technology, Vol. 206, Sept. 2020. DOI: 10.1016/j.ast.2020.106181.

8. Linden, A., “S-69 (XH-59A) Advancing Blade Concept Demonstrator,” Igor Sikorsky Historical Archives, Apr. 2013. https://www.sikorskyarchives.com/S-69%20(XH-59A).php.

9. Park. J., Kim, D., Chae, S., Lee, Y., and Go, J., “Vibration and Performance Analyses Using Individual Blade Pitch Controls for Lift-Offset Rotors.” International Journal of Aerospace Engineering, 2019. DOI: 10.1155/2019/9589415.

10. Ruddell, A.J. “Advancing Blade Concept (ABC) Technology Demonstrator.” U.S. Army Research and Technology Laboratories (AVRADCOM), 1981.

11. Ruddell, A. J. et al. “XH-59A ABC Technology Demonstrator Altitude Expansion and Operational Tests.” U.S. Army Research and Technology Laboratories (AVRADCOM), 1981.

12. “X2 Helicopter Technology,” Lockheed Martin, 2022. https://www.lockheedmartin.com/en-us/products/x2-helicopter-technology-demonstrator.html.

13. Zhang, J., Smith, E., Schmitz, S. “Vibration Reduction Using Individual Blade Pitch Controls for Lift-Offset Coaxial Rotor Vehicles at Low and High Speeds.” Transformative Vertical Flight, Santa Clara, CA, February 6-8, 2024. Vertical Flight Society, 2024.